Gianfranco Chicco, Roberto Napoli, Filippo Spertino

Performance Assessment of the Inverter-based Grid Connection of Photovoltaic Systems

The present trend towards extended adoption of energy production from renewable sources is leading to increased attention towards the diffusion of grid-connected photovoltaic (PV) systems. Different technologies are available for the connection of the PV systems to the grid through inverter-based Power Conditioning Units (PCUs). This paper presents the results of a comparative study referred to the characteristics of different types of PCUs, based on the experimental results obtained for a wide range of solar irradiance and operating conditions. The performance of the grid connection has been characterised by using a set of parameters, referred both to the DC and to the AC side of the inverter, such as the efficiency of the maximum power point tracking, the DC/AC efficiency, the power factor and the harmonic distortion of voltage and current at the interface with the grid. The PV systems have been further characterised by considering their ability of avoiding the undesired islanding operation through relatively fast detection of the islanding conditions and fast PV system shutdown. The results are discussed and compared to the specifications provided by the manufacturers and to the limits imposed by some standards.

Key words: grid connection, harmonic distortion, inverter, islanding, maximum power point tracking, photovoltaic systems, power conditioning unit, power quality

1 INTRODUCTION

In the last decades, the energy production from renewable sources has become an increasingly important subject, in a framework aimed at reducing the environmental pollution and at pushing forward the development of technologies for alternative production of energy. The economic barriers that are of obstacle to a widespread evolution of some types of energy production from renewable sources have often been reduced by offering specific incentives towards the construction and operation of new plants and systems. In this framework, Photovoltaic (PV) systems have been subject to special attention. However, the present size of most PV systems is still relatively limited and not sufficient to cover the entire local load. The size limitations make PV systems suitable to operate as local generators in peak-shaving mode, to reduce the load demand seen by the grid.

In addition to the clear environmental benefits, the effectiveness of using PV systems for energy production also depends on the technical characteristics of the connection of these systems to the distribution grid [1]. In particular, the PV systems are generally unable to ensure the properties of system controllability by acting as a single generation source for an island normally connected to the utility grid, and as such they must be rapidly disconnected whenever the grid is switched off (for islanding prevention), as well as in case of over/under voltage or over/under frequency. In these cases, suitable protections shutdown the PV system within time limits specified by specific Standards [2].

The PV system components can be schematically represented as in Figure 1. The DC side includes a number of arrays of PV modules, interfaced with the external grid by means of inverters or, more generally, Power Conditioning Units (PCUs). The main components of the PCU are the Maximum Power Point Tracker (MPPT), the DC/AC conver-
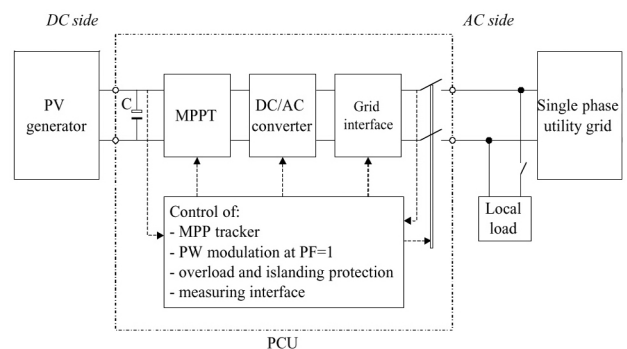

Fig. 1 Layout of a PV system connected to the single-phase grid

Table 1 **Power Conditioning Unit Specifications**

Unit	A	B	C	D
transformer	HF	LF	HF	LF
nominal DC power P_{DCn} (W)	2700	2770	2700	1600
MPPT voltage range ΔV_{MPPT} (V)	66–120	268–550	150–400	140–400
MPPT efficiency η_{MPPT}	99 %	99 %	99 %	99 %
nominal AC power P_{ACn} (W)	2500	2600	2500	1500
nominal efficiency η_{DC-AC}	93 %	94 %	93 %	93 %
power factor PF	1	1	1	1
THD of nominal AC current THD_I	–	4 %	3 %	4 %
run-on time t_I(ms)	10	200	–	200

ter, the internal protections and various control systems required for performing efficient PV system operation. The scope of the MPPT is to optimise the performance of the PV modules by tracking the maximum power point of the current/voltage characteristic with the highest possible accuracy, in function of the conditions affecting the DC power supplied (solar irradiance and temperature). In addition, the electrolytic capacitor C acts as buffering storage device to balance the fluctuations of the single-phase instantaneous power demand at the AC side, that occur at double frequency with respect to the grid frequency, in order to limit the DC voltage ripple at the input section of the PCU. The other controls are aimed at providing AC power supply with acceptable features in terms of high power factor and reduced waveform distortion [3]. In the presence of multiple PV systems operating in a close portion of the distribution system, the PV system interactions have to be specifically analysed [4, 5], since they could lead to malfunctioning of the controls, being each control typically designed on the basis of the individual PV system characteristics.

Various technologies are available for performing the DC/AC conversion [6, 7, 8, 9]. Self commutated inverters (with MOSFETs or IGBTs in bridge configuration) are equipped with Pulse Width Modulation (PWM) and High Frequency (HF) or Low Frequency (LF) transformer. Different solutions are also available for what concerns the number and location of the inverters in the PV system, including a *centralised* inverter for the whole array of PV modules, *string* inverters (one inverter for each string of PV modules connected in series) or *module integrated* inverters (a single inverter for each PV module) [10]. In particular, the adoption of module integrated inverters leads to some benefits, concerning system modularity, increased system availability, and minimisation of the losses due to mismatching of the current/voltage characteristics, because of the

individual and independent control of the single inverters. As a counterpart, the inverters integrated in the single modules must withstand the different climatic conditions that occur during the PV system operation and must be individually equipped with islanding protections.

This paper reports on the results of an experimental investigation carried out on a set of relevant technical aspects concerning the connection of PV systems to the external grid. A first aspect is the characterisation of the PCU performance by using a set of parameters, referred both to the DC and to the AC side of the inverter, such as the efficiency of the maximum power point tracking, the DC/AC efficiency, the power factor and the harmonic distortion of voltage and current at the interface with the grid [11]. A further aspect is the characterisation of the ability of the PV system to provide a relatively fast shutdown in order to avoid undesired islanding operation.

The investigation concerns four PV systems connected to the LV three-phase grid. For the sake of comparison, the systems have similar values of the total power (about 20 kW). All the PV plants have been funded by the Italian programme »10,000 PV roofs« [12] and are in operation since 2002.

The PV systems data are summarised in Table 1. Three PV systems (A, B and C) include six single-phase inverters, with groups of two inverters connected in parallel to each single phase. The PV system D includes eight single-phase inverters, with two groups of three inverters and one group of two inverters connected to the three-phase grid. The PWM inverters belong to different manufacturers. In particular, the inverters A and C use the HF transformer, whereas the inverters B and D adopt the LF toroidal transformer. For the sake of comparison, the active power is normalised with respect to the nominal DC power of the inverter.

2 EXPERIMENTAL TESTS FOR POWER QUALITY CHARACTERISATION

2.1 Definition of the parameters

A global view of the power quality issues has been considered for the experimental study, including the information available from measurements both at the DC side and at the AC side [13]. In particular:

- P_{DC} is the PV power, that is, the input power of the PCU;
- P_{AC} is the active power at the grid side;
- P_{MAX} is the maximum power calculated on the power-voltage $P(U)$ characteristic obtained by the transient charge of a capacitor (see subsection 2.2);
- U_{AC} is the RMS voltage at the AC side;
- I_{AC} is the RMS current at the AC side;
- I_k is the RMS value of the k-th harmonic order component of the AC current supplied to the load;
- U_k is the RMS value of the k-th harmonic order component of the AC voltage at the point of grid connection;
- n is an even number representing the highest harmonic order considered in the study.

The following parameters have been used for characterising the PCU performance in terms of power quality:

1. the *MPPT efficiency* is the parameter describing the optimum utilisation of the PV array [14]. It represents how close to the maximum power P_{MAX} the MPPT is operating and is expressed by

$$\eta_{\mathrm{MPPT}} = \frac{P_{\mathrm{DC}}}{P_{\mathrm{MAX}}} \qquad (1)$$

2. the *inverter efficiency* is defined in the conventional way as the ratio between the output and the input power

$$\eta_{inv} = \frac{P_{\mathrm{AC}}}{P_{\mathrm{DC}}} \qquad (2)$$

3. the *Total Harmonic Distortion* (THD) of the AC current

$$\mathrm{THD}_I = \frac{1}{I_1} \sqrt{\sum_{k=2}^{n} I_k^2} \qquad (3)$$

4. the THD of the AC voltage

$$\mathrm{THD}_U = \frac{1}{U_1} \sqrt{\sum_{k=2}^{n} U_k^2} \qquad (4)$$

5. the *power factor*

$$PF = \frac{P_{AC}}{U_{AC}\,I_{AC}}. \qquad (5)$$

2.2 Instrumentation

The experimental tests on the PV systems have been carried out in clear days, for a wide range of solar irradiance. The results analysed are extracted from daily measurements. The analysis has been performed by taking into account national and international standards, guidelines and specifications [15, 17, 18, 19]. A dedicated LabView [20] software has been used for automatic data acquisition. The software is based on a Data Acquisition board (DAQ), integrated into a notebook PC. The DAQ specifications are the sampling rate (500 kSa/s), the resolution of the Analogue Digital Converter (12--bit), the number of channels (8 differential channels) and a voltage range of ±10 V. Suitable voltage and current probes (used as a signal conditioning stage to extend the range of the measured quantities) must have operational amplifiers with both high input resistance (> 1 MΩ), in order to neglect the »loading effect«, and low output resistance (<50 Ω), for obtaining low time constants with the capacitance of the Sample & Hold circuit in the DAQ board. Typical uncertainty can be within ±0.1 % for voltage measurement, ±0.4 % for current measurement and about ±0.5 % for power measurement. These values have been obtained by performing a suitable calibration procedure, in the laboratory, on the measurement chain composed of DAQ and probes. Without this calibration, the uncertainty would be significantly higher (e.g., 1 % or more).

The software implements Virtual Instruments [21] behaving as storage oscilloscope and multimeter for measurement of RMS voltage (600 V), current (20 A), active power and power factor. The multimeter also performs harmonic analysis for the calculation of the Total Harmonic Distortion and operates as data logger with user-selected time interval between two consecutive measurements.

2.3 Tracing the PV generator current-voltage characteristic by transient charge of a capacitor

In order to measure in a single sweep the current-voltage $I(U)$ characteristic of a PV generator, proper measuring circuits of the first and the second order (with LC resonant components) can be used [15, 16]. Concerning the circuit of the first order, which gives the $I(U)$ only according to the generator operation, Figure 2 shows the scheme related to the method of the transient charge of capacitor (initially uncharged). The PV current, during the transient charge, is measured by a four-terminals shunt (or a current probe based on the Hall effect) and converted into a voltage signal, as well as the voltage across the PV generator.
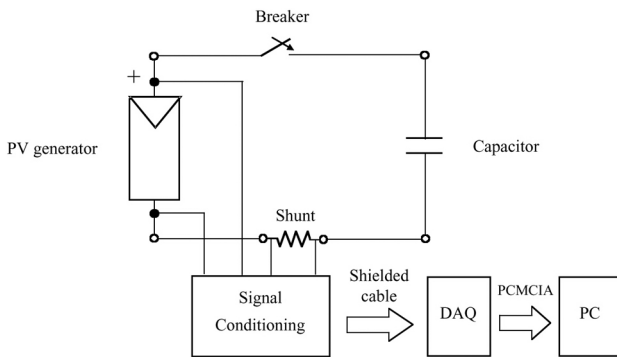
Fig. 2 Data acquisition system for tracing the I(U) characteristic of a PV generator

Fig. 3 Transient charge of a capacitor by a PV generator

Fig. 4 Current-voltage and power-voltage characteristics

The PV array can be seen as an equivalent generator. Depending on the operating point imposed by the load, this generator can be conveniently modeled by using the Norton generator (in the region of operation with almost constant current) or the Thévenin generator (in the region of operation with almost constant voltage), obtaining a linear approximation of the actual $I(U)$ characteristic. Then, the transient evolution associated to the capacitor charge can be divided into two parts. The first part can be studied as a capacitor charge with constant current and linear voltage, whereas the second part corresponds to a charge with a real voltage generator, leading to an exponential evolution of both voltage and current.

At the closing of the breaker, the voltage across the capacitor cannot change instantaneously and hence the PV generator changes abruptly its condition from open circuit to short circuit. Figure 3 shows that the current signal is, at first, enough constant and the corresponding voltage linear up to, roughly, the voltage of maximum power U_M (equal to almost 80 % of the open circuit voltage). The duration of this part of transient is approximately $\Delta t \approx \dfrac{C}{I_{SC}} U_M$, inversely proportional to the short circuit current I_{SC} and thus to the solar irradiance. Then, around the maximum power, the subsequent evolution is similar to an exponential, both for current and for voltage: also this duration depends directly on the capacitance.

During the transient charge, in which solar irradiance and temperature are considered constant, the $I(U)$ characteristic is covered in a single sweep from the short circuit to the open circuit condition.

For deeper understanding, it is necessary to mention the junction capacitance of PV generators, which has low value (much lower than microfarads), because an high number of series connections of PV cells (in the modules) and of PV modules (in
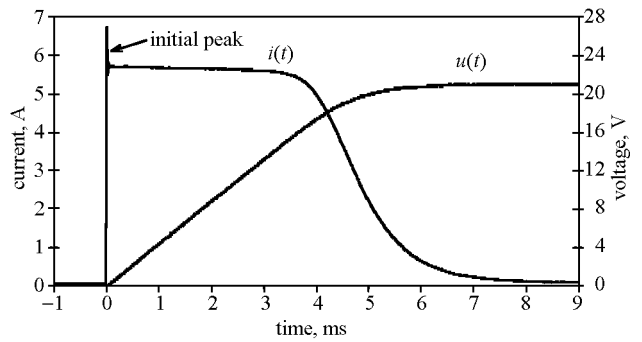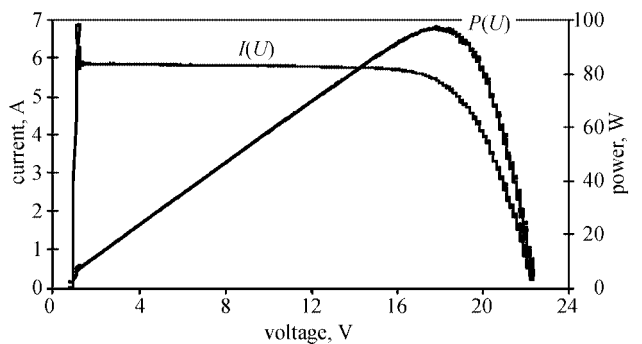
the strings) is often used to obtain the PV generator. Therefore a sharp peak of current, higher than the short circuit current, arises immediately, during the transient, when the voltage across the PV generator is shorted by the capacitor (Figure 3). With reference to the capacitance of capacitor, values within 1–5 mF can be suitable for obtaining transient durations within 5–100 ms, so that it is possible to neglect the interaction with the junction capacitance and assume constant solar irradiance and temperature.

The current-voltage curve of Figure 4 is obtained by plotting the values of current and voltage corresponding to the same time instant. In addition, multiplying the current values by the corresponding voltage gives the points of the power-voltage curve shown in Figure 4.

2.4 MPPT efficiency

The MPPT efficiency is obtained from two tests, carried out as close as possible in order to maintain similar ambient conditions (solar irradiance and temperature). The first test determines the current-voltage $I(U)$ and power-voltage $P(U)$ characteristic by the transient charge of a capacitor. The maximum power P_{MAX} is determined from the complete $I(U)$ and $P(U)$ curves (Figure 4). The second test determines the power $p_{DC}(t)$ as product of the DC

190

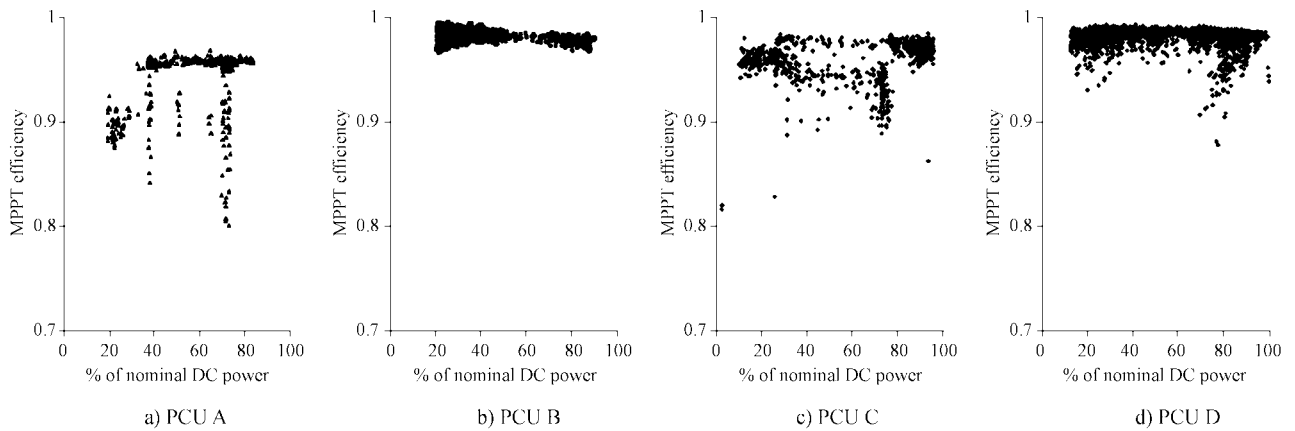a) PCU A   b) PCU B   c) PCU C   d) PCU D

Fig. 5   MPPT efficiency for the PCUs tested

voltage $u_{DC}(t)$ and current $i_{DC}(t)$ signals of the inverter. Since the AC single-phase load demands an instantaneous power fluctuating at double frequency with respect to the grid frequency, voltage and current exhibit a 100 Hz ripple, evaluated as the peak to peak values $2\sqrt{2}\,U_{2k}$ and $2\sqrt{2}\,U_{2k}$ with respect to the mean values U_0 and I_0, respectively, for $k = 1,\ldots,n/2$. The ripple voltage and the ripple current always have a 180° phase shift, that is, on the $I(U)$ characteristic, if voltage increases, then current decreases. On the other hand, ripple voltage and ripple power can have a 0° or 180° phase shift, respectively if the operating points on the $P(U)$ characteristic are biased on the left ($dP/dU > 0$) or on the right ($dP/dU < 0$) with respect to the MPP. If the operating points on the $P(U)$ characteristic are not biased, it is difficult to state the phase shift of $p_{DC}(t)$ with respect to $u_{DC}(t)$. The ripple power must be as low as possible, because it decreases the mean value (active power P_{DC}) with respect to the maximum value. The expression of the power P_{DC} is

$$P_{DC} = U_0 I_0 + \sum_{k=1}^{n/2} U_{2k} I_{2k} \cos \varphi_{2k} \qquad (6)$$

where $\cos\varphi_{2k}$ is negative, so that P_{DC} is lower than the product $U_0 I_0$. An approximation (in excess) of the MPPT efficiency can be provided by measuring the DC signals with the peak value of $p_{DC}(t)$ assumed as P_{MAX}, without determining the whole $P(U)$ characteristic. The MPPT efficiency values shown in Figure 5 have been obtained by repeating the measurement of μ_{MPPT}, carried out by the above mentioned approximation, for different conditions of P_{DC} (corresponding to different values of the solar irradiance).

There are various causes that may decrease the MPPT efficiency, the main ones being:

a) the adoption of *simplified* MPPT strategies;

b) the presence of *overload* due to high solar irradiance or high inverter temperature;

c) the *shading effect* on some modules of the PV array.

About MPPT strategies, an example is shown where the MPPT of the PCU A imposes the operation at fixed voltage (about 80 % of U_{OC}), where the open-circuit voltage U_{OC} of the PV array is assesses by means of a fast open-circuit measurement at time intervals of about two seconds (e.g., Figure 6). This practice does not correspond to searching for the true MPP, and as such it leads to relatively low values of the MPPT efficiency.
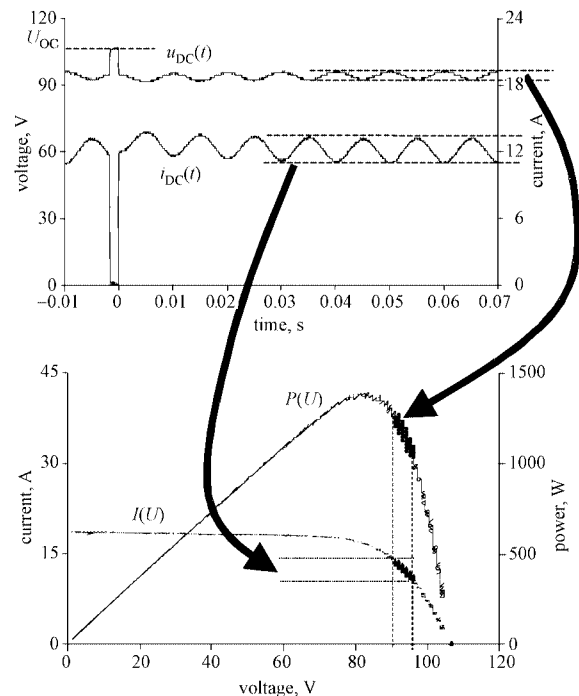

Fig. 6 Voltage and current ripples at the DC side in the presence of overloading
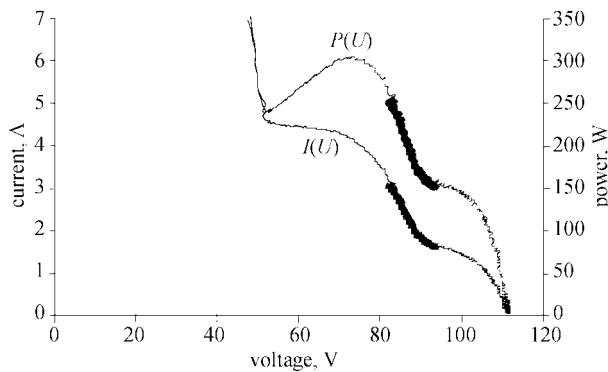
Fig. 7 Operating points imposed by the MPPT in the presence of the shading effect
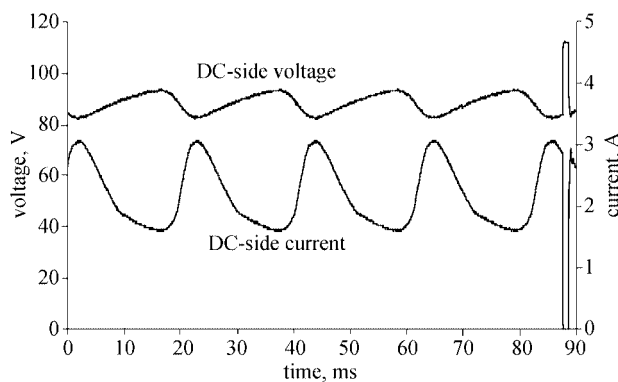

Fig. 8 Voltage and current ripples at the DC side in the presence of shading effect

An example of overload is shown in Figure 6 for the same PCU A. In overload conditions, the MPPT is intentionally disabled, so that the operating point moves away from the MPP, reaching locations at higher voltages with respect to the one corresponding to the MPP, in a region of the $I(U)$ characteristic with high (negative) slope and resulting high amplitude of the current ripple.

For what concerns the shading effect, tests carried out on a façade PV plant with the inverter A have put into evidence a partial shading effect occurring during morning periods in part of the year (from April to September) [22]. This shading effect, concentrated on some cells of a PV array, determines a mismatch of cell current-voltage $I(U)$ characteristics, with an important reduction of the available power, only limited by the bypass diodes, i.e., diodes connected in anti-parallel to a group of PV cells in order to limit the negative impact of the shading effect. Furthermore, the shaded cells can work as a load and the hot spots can rise. In order to evaluate the PCU performance in shading conditions, experimental data have been collected. As shown in Figure 7, representing the right-hand sides of the complete $P(U)$ and $I(U)$ characteristics, the $P(U)$ characteristic changes shape and can exhibit more than one maximum power point. More specifically, the maximum power corresponds to a voltage lower than the operating voltage range of the MPPT indicated in Table 1. Then, very high amplitudes of the peak-to-peak voltage and current ripples occur (Figure 8) with operating points even located far from the local maximum (Figure 7) and the MPPT efficiency falls down considerably.

2.5 DC/AC efficiency

Figure 9 shows the DC/AC efficiency values for the PCUs tested. The PCUs B and D, with LF toroidal transformer, generally exhibit better performance than the inverters with HF transformer. The PCU B, which exhibits the best performance, has high nominal power and DC voltage within the range 300–350 V, allowing for selecting the turns ratio of the transformer close to unity to obtain the peak value of the grid voltage $U_p = \sqrt{2}U_r \cong 325$ V (with single-phase nominal voltage $U_r = 230$ V). The PCU B maintains high DC/AC efficiency also at low DC power ($P_{DC} < 30$ % of nominal DC power), where

a) PCU A

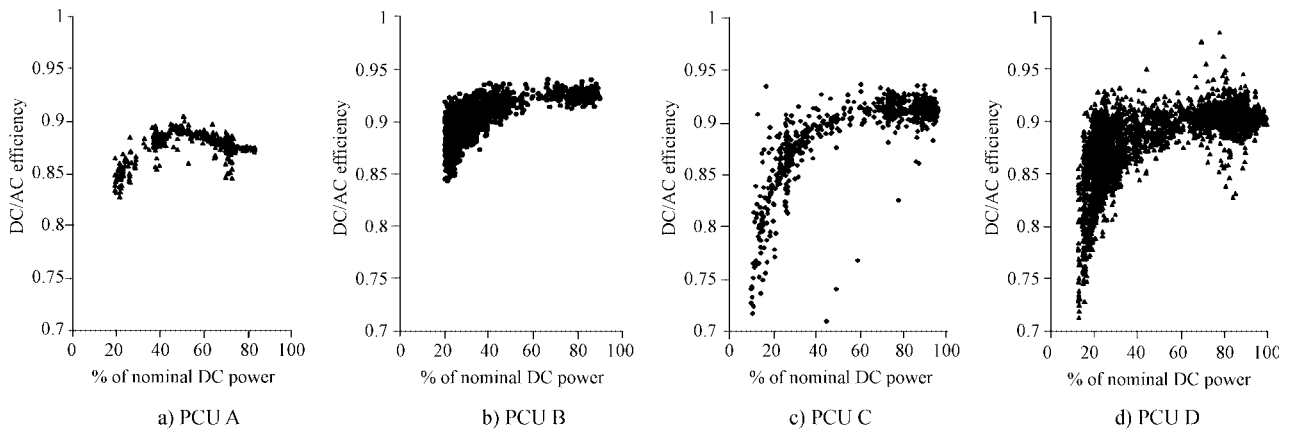b) PCU B

c) PCU C

d) PCU D

Fig. 9 DC/AC efficiency of the PCUs tested

there is a large number of hours of operation. On the other hand, the PCU D operates at a lower voltage level, i.e., in the range 150–190 V. Moreover, the PCU D has a larger spread of the DC/AC efficiency values due to a wider range of operating conditions, also including overloads caused by high solar irradiance. The relatively lower efficiency of the PCU A is also affected by the systematic shading effect, as shown in the previous subsection, that also produces even harmonics of the AC current; even harmonics are not present in the AC voltage and thus do not contribute to the AC active power production. The PCU C is able to guarantee high DC/AC efficiency at high power, but its efficiency falls down when the power decreases.

2.6. Total Harmonic Distortion

From the power quality point of view, the grid connection of PV plant through inverter implies the presence of distorted current waveforms, even if the voltage at the grid side has negligible distortion when the PV plant is not connected (open connection). The presence of a distorted voltage waveform

in the open connection leads to the modification of the harmonic spectrum when the PV plant is connected [25]. Clearly, the nature of the current distortion, represented by the most involved harmonic orders, varies from case to case and during time. The worst power quality conditions may occur at low loading [23, 24], but in these cases the current magnitudes are relatively low and do not cause significant problems.

The Total Harmonic Distortion (THD) values of the AC currents are shown in Figure 10. The PCU A has a poor harmonic behaviour, since the THD of its currents never falls below 8 %. The other PCUs exhibit decreasing values for increasing values of the DC power. The THD of the currents for the PCUs C and D show variations in a relatively large range, whereas the THD of the voltage remains close to the same values, as shown in Figure 11.

The PCU D presents a particular behaviour, with the presence of high current THD spots at high power. These spots are due to the effect of the network impedance measurement circuit, based on the
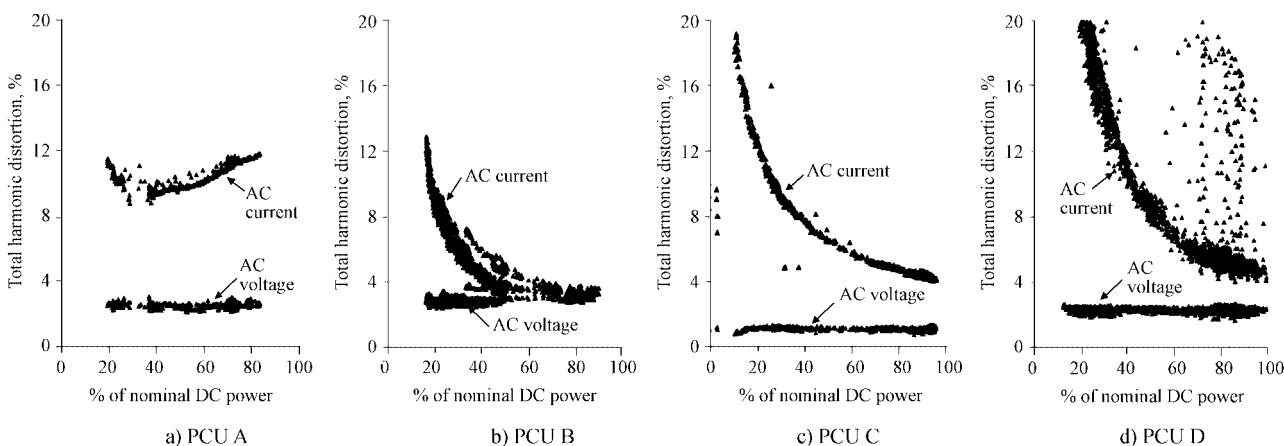

a) PCU A   b) PCU B   c) PCU C   d) PCU D

Fig. 10 Total Harmonic Distortion of the current for the PCUs tested

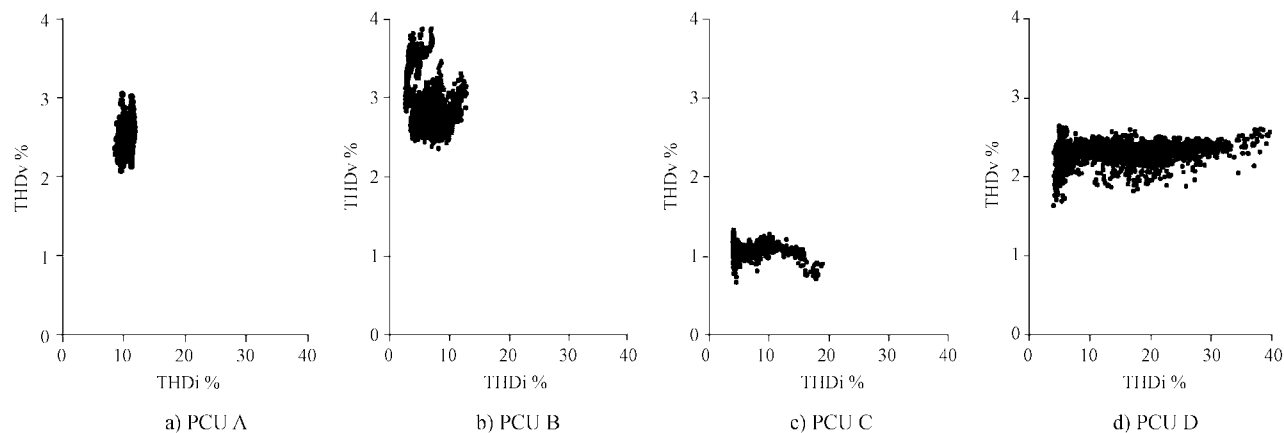a) PCU A   b) PCU B   c) PCU C   d) PCU D

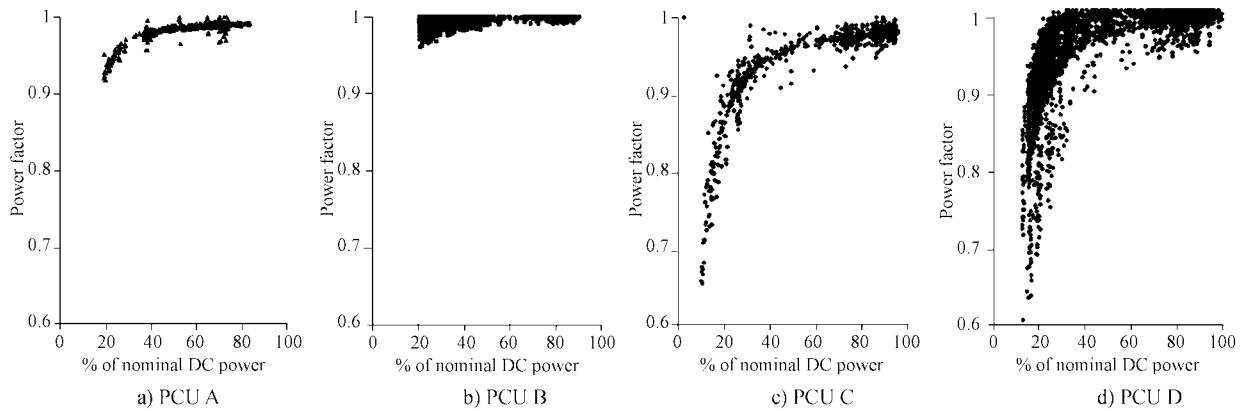Fig. 11 Current vs. voltage Total Harmonic Distortion for the inverters tested

Fig. 12 Power factor of the PCUs tested

temporary switching of a RC circuit at time cadence of about 5 s. This technique, used for islanding detection [26], produces distortion to the current waveform, deteriorating the current THD. The number of spots detected depends on the time cadence with which the measurements are performed (12 s in this case) and on the length of the time interval used to compute the THD (100 ms). The lack of synchronism between harmonics measurement and network impedance measurement determines the possible presence of capacitive peaks in the current waveform sampled for performing harmonic analysis.

The PCU B exhibits better characteristics with respect to the other PCUs, since the THD of its currents remains relatively low even in the presence of the largest distortion of the voltage, for the entire range of normalised DC powers.

In order to check the fulfilment of the maximum limits allowed for the waveform distortion, Figure 10 shows that the PCUs B and C, as well as the PCU D in most of the cases, satisfy the requirement of current THD lower than 5 % at full load imposed by [18], while the PCU A never reaches the required level. However, from the experimental results it is clear that the indications concerning the harmonic distortion should be more specifically referred to the voltage THD and possibly to various power levels.

2.7 Power Factor

The power factor embeds the contributions of both the phase shift between current and voltage at the fundamental frequency, and the harmonic distortion of the waveforms. All the PCUs tested exhibited a qualitatively similar behaviour above 50 % of the nominal DC power (Figure 12). However, the PCUs C and D exhibit significant reductions of the power factor at low DC power. In particular, the power factor values for the PCUs C and D are lower than the ones proposed by some standards, e.g., the IEEE Standard 929–2000, according to which the PV system should operate at power factor higher than 0.85 when the output exceeds 10 % of the rating [27]. Furthermore, the PCU C presents low power factor but relatively low harmonic distortion content, so that the power factor reduction in this case has to be associated to a scarcely effective phase angle control.

3 AVOIDING THE ISLANDING OPERATION

Islanding operation occurs when, in the absence of supply from the utility grid, the PV plant operates alone to supply the local load. When an island is formed, frequency and voltage may exceed the acceptable ranges, so that frequency and voltage monitoring can recognise the island formation and can switch the PV plant off. However, in case of sufficient balance of generation and load, the monitored quantities may fall into a range for which the protections are unable to work (the non-detection zone) and the island could persist without trip of the protections. Hence, efficient islanding detection must include the addition of specific functions to the common protection schemes, e.g., measurement of the network impedance. Phase criteria based on the detection of zero phase error between the PV output current and the voltage at the PV terminals have been illustrated in [28] in order to reduce the size of the non-detection zones. A further phase-shift method is illustrated in [29]. Different functions have been tested in [30] on typical circuits for islanding protection. However, several test circuits have been proposed in the literature and the standardisation of the criteria for islanding detection is still in progress [26, 30].

The typical parameter representing the ability of automatic shutdown of the PCU after a lack of supply at the utility side of the network is called *run-on* time [31, 32] and consists of the time elap-

sed between the instant of utility disconnection and the instant at which the interruption of the current supplied from the PV system has been completed.

A typical categorisation of the islanding events leads to identifying *short-term* (< 1 s) and *long-term* (> 1 s) islanding operation. Long-term islanding operation has to be avoided, mainly for ensuring the system safety. In fact, during islanding the maintenance or repair personnel, arriving to operate on an expected isolated feeder, could be unaware that it is still energised and could then be injured. In addition, after opening the circuit breaker from the utility side, the islanded PV system would lose synchronism with respect to the utility. The analysis of PV system islanding also requires to take into account the possible mutual interference among the islanding prevention methods, that could lead to longer run-on times and possible failure to detect islanding if several PV systems are present in the island.

The islanding tests have been carried out by performing measurements at the AC side of each single inverter. Concerning the PV system protection, some national specifications [33] require introducing redundant islanding protections, with both the local protection at the (output) AC side of each inverter and a centralised protection for the three-phase system at the grid side. The presence of these protections impacts on the time evolution of the shutdown process.

The run-on time has been evaluated by using the circuit of Figure 13. The run-on time evaluation has been carried out in the worst case, where the active powers of inverter and load are equal, $P_{AC} = P_{load}$, and the reactive power is null. This worst case corresponds to the *matching condition*: at the moment in which the grid is switched off, the current supplied by the inverter has the same RMS value as the current of the local load, thus making it difficult to detect the islanding condition and to deactivate the PV system. In case of different RMS

currents between inverter and load, the release of relays is easier, since an over-voltage or under-voltage occurs after the grid de-energisation.

The average values of the run-on times occurred on a set of tests are around 7 ms for the PCU A, 120 ms for the PCUs B and D, and 60 ms for the PCU C. For the PCU A, Figure 14 shows that the PCU switch-off is very fast (6 ms), in line with the values specified in Table 1. Its run-on time could even be too fast with respect to the switch-off duration required by most standards (about 200 ms), leading to possible untimely trip. For the PCU B, Figure 15 and Figure 16 show the time evolution of the load current and of the voltage at the terminals of the circuit breaker, respectively in case of measurement on the phase and on the neutral pole of the circuit breaker. The run-on time is 84 ms for the case in Figure 15 and 80 ms for the case in Figure 16. Both cases are within the inverter specifications shown in Table 1. However, in a few cases one of the inverters of the PCU B exhibited run-on times up to 280 ms, exceeding the manufacturer's specifications (200 ms). The time evolution of the switch-off for the PCU C is shown in Figure 17 for a run-on time of 63 ms. The PCU D has simi-
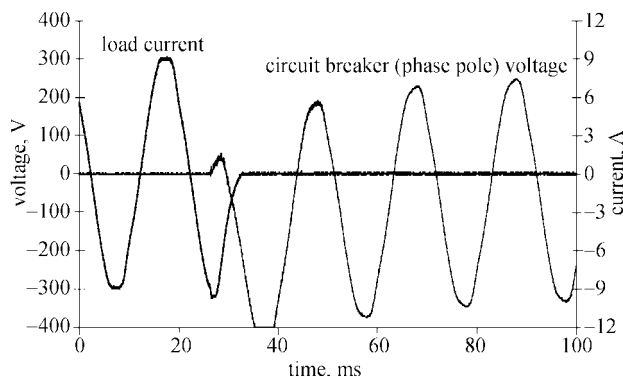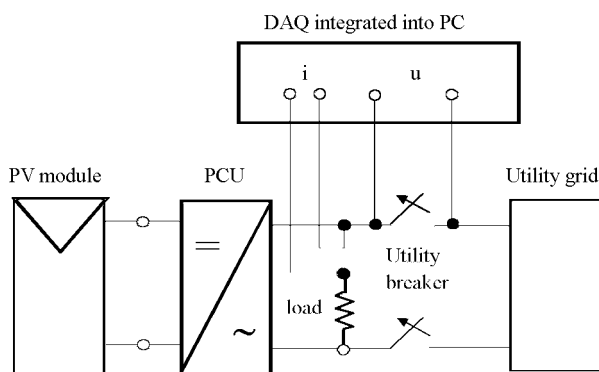

Fig. 14 Shutdown test results on the PCU A
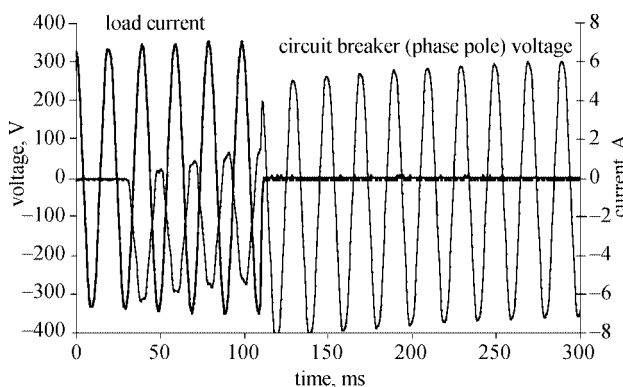

Fig. 13 Circuit for the islanding time detection

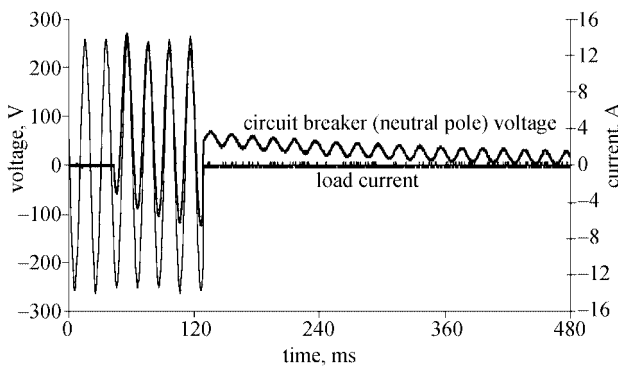Fig. 15 Shutdown test results on the PCU B

Fig. 16 Shutdown test results on the PCU B (voltage measurement on the neutral pole)
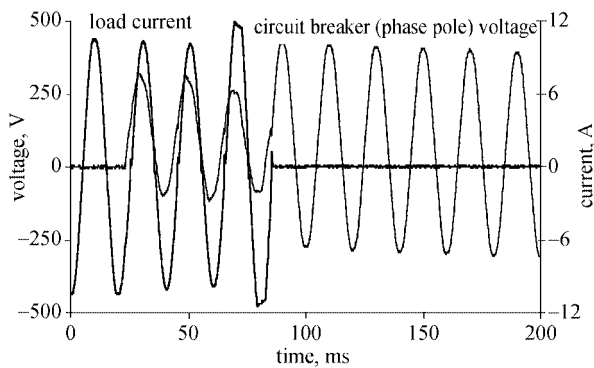

Fig. 17 Shutdown test results on the PCU C

lar characteristics as the PCU B and exhibited a similar behaviour. The asymmetrical evolution of the voltage, shown in all the cases after the load current interruption, is due to the presence of the RC transient consequent to the discharge of the capacitor connected at the AC inverter terminals.

4 CONCLUSIONS

This paper has presented detailed results concerning the performance of inverter-based PCUs, obtained from an extended experimental analysis. A suitable set of measured quantities has been selected, in order to perform a widespread quality testing of the PCUs. The results of the measurements carried out in actual operating conditions of the PV systems have put into evidence some critical aspects in the performance of the various PCUs. These aspects are mainly linked to the internal strategies implemented for tracking the maximum power point and to possible severe conditions occurring during the actual operation for solar irradiance, temperature, possible shading effect and distortion of the voltage waveform at the point of grid connection. The results obtained show that the performance of PCUs with similar rated values can be significantly different. In some cases, either the de-

clared specifications or the limits imposed by specific standards were not completely satisfied. These facts should be carefully taken into account by the manufacturers, in order to define suitable inverter and PCU specifications. In particular, the procedures for PCU testing based on the results obtained from laboratory tests could be refined to better reflect the PV system behaviour in real conditions.

REFERENCES

[1] S. A. Papathanassiou, N. D. Hatziargyriou, **Technical Requirements for the Connection of Dispersed Generation to the Grid**. Proc. IEEE/PES Summer Meeting 2, July 15–19, 2001, 749–754.

[2] ..., **IEEE Standard for Interconnecting Distributed Resources with Electric Power System**, Std. 1547–2003, 28 July 2003.

[3] M. Prodanovic, T. C. Green, **Control and Filter Design of Three-phase Inverters for High Power Quality Grid Connection**. IEEE Trans. on Power Electronics 18, 1, Jan. 2003, 373–380.

[4] J. H. R. Eslin, W. T. J. Hulshorst, A. M. S. Atmadji, P. J. M. Heskes, A. Kotsopoulos, J. F. G. Cobben, P. Van der Sluijs, **Harmonic Interaction Between Large Numbers of Photovoltaic Inverters and the Distribution Network**. Proc. IEEE Bologna Power Tech, June 23–26, 2003.

[5] D. G. Infield, P. Onions, A. D. Simmons, G. A. Smith, **Power Quality from Multiple Grid-Connected Single-Phase Inverters**. IEEE Trans. on Power Delivery 19, 4, October 2004, 1983–1989.

[6] F. Sick, T. Erge, **Photovoltaics in Buildings: a Design Handbook**. International Energy Agency, 1996.

[7] H. Wilk, R. Hotopp et al., **Photovoltaic Systems**. The Fraunhofer Institute for Solar Energy, Comett Book, 1995.

[8] P. Rooij, **Technical Evaluation of Modern Grid Connected Inverters**. Proc. PV in Europe: from PV technology to energy solutions, Roma, Italy, October 2002, 868–871.

[9] E. T. Schönholzer, **Inverters for Utility Interactive Photovoltaic Power Plants**. Proc. Melecon 1989, April 11–13, 1989, 16–20.

[10] A. Abete, F. Scapino, F. Spertino, **Comparison of Power Quality Between Centralised Inverters and Module Integrated Inverters in Grid Connected PV Systems**. Proc. 17th European Photovoltaic Solar Energy Conference, Munich, Germany, October 2001, 421–425.

[11] A. D. Simmons, D. G. Infield, **Current Waveform Quality from Grid-connected Photovoltaic Inverters and its Dependence on Operating Conditions**. Progress in Photovoltaic 8, 2000, 411–420.

[12] S. Castello, M. Garozzo, S. Li Causi, A. Sarno, **The Italian Roof-top Program: Current Status and First Results**. Proc. 17th European PV Solar Energy Conference, Munich, Germany, October 2001, 888–891.

[13] G. Chicco, R. Napoli, F. Spertino, **Experimental Evaluation of the Performance of Grid-connected Photovoltaic Systems**. Proc. IEEE Melecon 2004, Dubrovnik, Croatia, May 12–15, 2004, 3, 1011–1016.

[14] M. A. S. Masoum, H. Dehbonei, E. F. Fuchs, **Theoretical and Experimental Analyses of Photovoltaic Systems with Voltage- and Current-based Maximum Power-point Tracking**, IEEE Trans. on Energy Conversion 17 (4) December 2002, 514–522.

[15] ..., Commission of the European Communities, Joint Research Centre, Guidelines for the Assessment of Photovoltaic Plants – Initial and Periodic Tests on PV Plants, Ispra, Italy, 1995.

[16] ..., **European Norm EN 60904-1**, Photovoltaic Systems: Measurement of the Current-voltage characteristics, 1994.

[17] ..., International Electrotechnical Commission (IEC), **Limits for Harmonic Current Emission (equipment input current ≤ 16 A per phase)**, IEC 61000-3-2, 2000.

[18] ..., International Electrotechnical Commission, **Photovoltaic Systems: Characteristics of the Utility Interface**, IEC Standard 1727, 1995.

[19] A. R. Oliva, J. C. Balda, **A PV Dispersed Generator: a Power Quality Analysis within the IEEE 519**, IEEE Trans. on Power Delivery 18, 2 (April 2003) 525–530.

[20] ..., National Instruments, **LabView 7 Express User Manual**. April 2003.

[21] A. Abete, G. Bergamasco, L. Ferraris, F. Spertino, **A Measuring Procedure to Assess the Inverter Performance for Grid-connected Photovoltaic Systems**. Proc. 9th EPE, Graz, Aug. 2001.

[22] G. Graditi, F. Spertino, S. Li Causi, **Shading Effect on MPPT Performance in a Grid Connected 20 kWp PV System**. Proc. 19th European Photovoltaic Solar Energy Conference, Paris, France, 7–11 June 2004, 2254–2257.

[23] A. R. Oliva, J. C. Balda, D. W. McNabb, R. D. Richardson, **Power-quality Monitoring of a PV Generator**. IEEE Trans. on Energy Conversion 13, 2 (June 1998) 188–193.

[24] A. Abete, R. Napoli, F. Spertino, **Field Tests During the Installation of a 20 kWp Grid-connected PV System**. Proc. PV in Europe: from PV technology to energy solutions, Rome, October 2002, 1069–1072.

[25] G. Chicco, J. Schlabbach, F. Spertino, **Characterisation and Assessment of the Harmonic Emission of Grid-Connected Photovoltaic Systems**. IEEE St. Petersburg Power Tech, St. Petersburg, Russia, June 27–30, 2005.

[26] D. Schulz, R. Hanitsch, **Islanding Detection in Germany: Current Standards and Development**. Proc. 17th European PV Solar Energy Conference, Munich, Germany, Oct. 22–26, 2001, 520–523.

[27] ..., The Institute of Electrical and Electronics Engineers, **IEEE Recommended Practice for Utility Interface of Photovoltaic (PV) Systems**. IEEE Std. 929-2000, 3 April 2000.

[28] M. E. Ropp, M. Begovic, A. Rohatgi, G. A. Kern, R. H. Bonn, S. Gonzales, **Determining the Relative Effectiveness of Islanding Detection Methods Using Phase Criteria and Nondetection Zones**. IEEE Trans. on Energy Conversion 15, 3, Sept. 2003, 290–296.

[29] G.-K. Hung, C.-C. Chang, C.-L. Chen, **Automatic Phase-shift Method for Islanding Detection of Grid-connected Photovoltaic Inverters**. IEEE Trans. on Energy Conversion 18, 1, March 2003, 169-173.

[30] A. Woyte, R. Belmans, J. Nijs, **Testing the Islanding Protection Function of Photovoltaic Inverters**. IEEE Trans. on Energy Conversion 18, 1 (March 2003) 157–162.

[31] M. E. Ropp, M. Begovic, A. Rohatgi, **Prevention of Islanding in Grid-connected Photovoltaic Systems**. Progress in Photovoltaics: Research and Applications 7, 1999, 39–59.

[32] M. Begovic, M. E. Ropp, **Determining the Sufficiency of Standard Protective Relaying for Islanding Prevention in Grid-connected PV Systems**. Proc. 2nd World Conference on PV energy conversion, Vienna, Osterreich, 1998, 2519–2522.

[33] ..., ENEL Distribuzione, **Criteri di allacciamento di tetti fotovoltaici alla rete BT di distribuzione** (Criteria for connecting photovoltaic roofs to the LV distribution system). DK 5950 specification (in Italian), March 2002.

Analiza svojstava izmjenjivačkih mrežnih priključaka fotonaponskih sustava. Sadašnji trend koji vodi prema sve većoj potrebi za proizvodnjom energije iz obnovljivih izvora energije usmjerava povećanu pozornost prema primjeni fotonaponskih (PV) sustava spojenih u mrežu. Različite su tehnologije raspoložive za spajanje PV sustava na mrežu preko izmjenjivačkih energetskih jedinica (PCU). Ovaj rad prikazuje rezultate usporednog proučavanja karakteristika različitih tipova izmjenjivačkih energetskih jedinica (PCU) na osnovi eksperimentalnih rezultata dobivenih za široki opseg Sunčeva zračenja i uvjeta rada. Svojstva mrežnog spoja okarakterizirana su korištenjem skupa parametara koji se odnose i na istosmjernu (DC) i na izmjeničnu (AC) stranu izmjenjivača, kao što su efikasnost praćenja točke maksimalne snage, DC/AC efikasnosti, faktor snage i harmoničko izobličenje napona i struja na spoju s mrežom. Fotonaponski sustavi su dalje okarakterizirani uzimajući u obzir njihove sposobnosti izbjegavanja neželjene operacije otočnoga rada njegovom relativno brzom detekcijom i isključivanjem. Provedena je rasprava o rezultatima, a zatim su rezultati uspoređeni sa specifikacijama dobivenim od proizvođača i s ograničenjima proisteklima iz nekih standarda.

Ključne riječi: mrežni spoj, harmonička izobličenja, izmjenjivač, otočni rad, praćenje točke maksimalne snage, fotonaponski sustavi, izmjenjivačka energetska jedinica, kvaliteta snage

AUTHORS' ADDRESSES

Prof. Gianfranco Chicco
Prof. Roberto Napoli
Ing. Filippo Spertino

Dipartimento di Ingegneria Elettrica, Politecnico di Torino
Corso Duca degli Abruzzi 24, 10129 Torino, Italy

Phone +39 011 564 7141
FAX +39 011 564 7199
E-mail: gianfranco.chicco@polito.it
         roberto.napoli@polito.it
         filippo.spertino@polito.it